Available online at www.sciencedirect.com
ScienceDirect
Journal of Sound and Vibration 304 (2007) 845–862
JOURNAL OF SOUND AND VIBRATION
www.elsevier.com/locate/jsvi

Positioning and tuning of viscous damper on flexible structure

K. Engelen*, H. Ramon, W. Saeys, W. Franssens, J. Anthonis

Laboratory of Agro-Machinery and Processing, Division of Mechatronics, Biostatistics and Sensors, Department of Biosystems, Katholieke Universiteit Leuven, Kasteelpark Arenberg 30, 3001 Leuven, Belgium

Received 5 October 2006; received in revised form 14 March 2007; accepted 19 March 2007
Available online 8 May 2007

Abstract

The complex eigenvalues of a flexible structure including a viscous damper are derived by solving the root locus of a transfer function that is composed of very easily identifiable parameters: the static stiffness of the structure at the damper location, the resonance frequencies of the undamped structure and the resonance frequencies of the structure in which the damper is replaced by a rigid link. Approximate solutions are proposed for the complex eigenvalues and formulas are derived for the maximum modal damping ratio and the optimal damping constant. The correctness of the formulas is illustrated by numerical examples of a cantilever beam with attached viscous damper. Although approximate solutions exist which are not restricted to the case of a single damper, these are only accurate when the difference between the undamped and constrained eigensolution is sufficiently small, while the approximations obtained in the present paper are accurate in a broader range without losing simplicity.

1. Introduction

Improving the dynamic behavior of flexible structures with low inherent damping is a research topic that has been given considerable attention in the last decades, especially in the fields of spacecraft dynamics [1] and dynamics of buildings and bridges [2]. It has been shown that incorporation of viscous dampers in the structure can be a very effective means of reducing unwanted vibrations [2]. From a design point of view, this means two questions have to be answered: (I) what are good locations for placing the dampers in the structure and (II) what are the optimal damping constants resulting in minimized vibrations.

In answering these questions, one starts generally from a discrete model of the structure, for example by means of finite elements. When the excitation mechanisms are known, forced responses can be performed for different locations and sizes of the dampers, hereby searching for an optimal configuration that minimizes structural responses like for example displacements, accelerations or internal forces. An other criterium that is often employed in the design of dampers consists of maximizing the damping level in specific vibration modes. This is certainly interesting when the excitation mechanisms are not well understood and the problematic modes are known.

*Corresponding author. Tel.: +32 16328527; fax: +32 16328590.
E-mail address: kurt.engelen@biw.kuleuven.be (K. Engelen).

0022-460X/$ - see front matter © 2007 Elsevier Ltd. All rights reserved.
doi:10.1016/j.jsv.2007.03.020

In both of the previously described approaches for designing dampers, the complex eigenvalues are required and in the case of the forced response also the complex mode shapes have to be known. These can both be obtained by solving the complex eigenvalue problem corresponding to free vibrations of the structure. However, repeatedly solving this complex eigenproblem for different damper locations and different damping constants can be very time consuming for structures with a large number of degrees of freedom. Therefore, Main and Krenk [3] suggest an approximate solution that requires solving only two real-valued eigenproblems for each damper location: the eigenproblem of the undamped structure and the eigenproblem of the structure in which each damper is replaced by a rigid link, corresponding to a damping constant of, respectively, zero and infinity. The solutions for intermediate values of the damping constant are approximated by an interpolation between the solutions for these two limiting cases. An explicit form of the approximate solution is obtained for the case the difference between the two solutions is sufficiently small, and an iterative scheme is proposed for the case where this difference is larger. Similar approximate solutions have been derived for various continuous structures such as a taut cable [4] and a simply supported beam [5]. Høgsberg and Krenk [6] recently used this two-component representation technique to study active control algorithms for collocated systems.

In this paper, an alternative approach is suggested to obtain the complex eigenvalues for the case where only one damper is implemented in the structure. It also starts from the solutions of the two limiting eigenvalue problems of the structure without and with locked damper, however, the root locus technique is applied to obtain results for intermediate values of the damping constant. Approximate expressions are obtained for the maximal attainable modal damping at a given damper location and the corresponding optimal damping constant. The only parameters in these expressions are the stiffness of the structure at the damper location and the resonance frequencies of the structure without and with locked damper. These parameters are easily obtainable from any commercial finite element package that is able to perform static and modal analysis. Besides, these parameters are also easily experimentally identifiable, making them very useful in practical design. The correctness of the formulas is verified for two numerical examples: a cantilever Bernouilli–Euler beam equipped with a translational viscous damper and a rotational viscous damper. Beam elements are simple elements, representative for many real systems and are often used to investigate the dynamic behavior of flexible structures with attached viscous dampers [5,7,8].

The formulas for the maximum modal damping and optimal damping constant derived here are similar to those derived by Preumont [1] for active control of structures with collocated sensors and actuators applying integral force feedback (IFF), i.e. the position is controlled as the integral of the force, which in fact is equivalent to viscous damping. Krenk [4] and Main and Jones [9] derived similar formulas for the special case of a taut cable with a viscous damper attached near the end. Main and Krenk [3] found approximate solutions for the damping constant that maximizes the decay rate of a general discrete structure with viscous dampers, which is only slightly different from the damping constant that maximizes the modal damping ratio. Previously published research results are compared with the results of this paper in Section 5.

2. Transfer function for collocated systems

In this section, the transfer function between the force f exerted on a flexible structure and its collocated displacement x is derived. Collocated means that the displacement at the location of the applied force is considered (Fig. 1a). This transfer function will be used in the subsequent section to find the eigenvalues of a viscously damped structure by solving a root locus problem. First the eigenvalues of an undamped structure are derived, which are used to construct the transfer function.

2.1. Eigenvalues of an undamped structure

The free response of an undamped discrete linear structure with n degrees of freedom is governed by the equations of motion

$$\mathbf{M}\ddot{\mathbf{q}} + \mathbf{K}\mathbf{q} = 0, \tag{1}$$

where $\mathbf{M}$ and $\mathbf{K}$ are the $n \times n$ mass and stiffness matrices and $\mathbf{q}$ is the $n \times 1$ vector of generalized displacements.

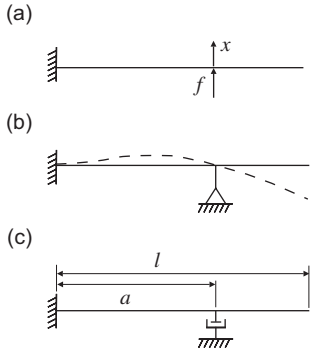

Fig. 1. (a) Cantilever beam with applied force and collocated displacement; (b) mode shape of cantilever beam with additional restraint; (c) cantilever beam with attached viscous damper.

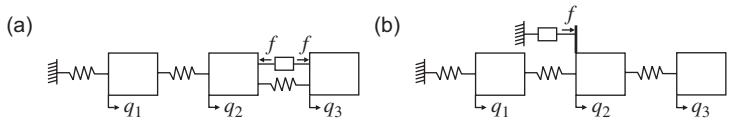

Fig. 2. Three mass system excited by an actuator acting on (a) relative motion and (b) absolute motion.

Assuming solutions of the form $\mathbf{q} = \mathbf{u}e^{st}$, yields the eigenvalue problem

$$(\mathbf{M}s^2 + \mathbf{K})\mathbf{u}_i = 0. \tag{2}$$

Non-trivial solutions are found by solving the characteristic equation

$$\det(\mathbf{M}s^2 + \mathbf{K}) = 0, \tag{3}$$

where the eigenvalues $s = \pm \mathrm{j}\Omega_i$ are purely imaginary in case of an undamped structure, Ω_i are the resonance frequencies of the structure and $\mathbf{u}_i$ are the corresponding modeshapes.

2.2. Transfer function for collocated systems

When an undamped structure is excited by a single force, the equations of motion can be written as follows:

$$\mathbf{M}\ddot{\mathbf{q}} + \mathbf{K}\mathbf{q} = \mathbf{b}f, \tag{4}$$

where $\mathbf{b}$ is the $n \times 1$ influence vector, which indicates the location and orientation of the point of excitation in the structure. For example, the influence vector of the three mass system of Fig. 2 is $\mathbf{b} = [0 \;\; -1 \;\; 1]^{\mathrm{T}}$ in the case where the actuator forces a relative motion of the masses, while it is $\mathbf{b} = [0 \;\; 1 \;\; 0]^{\mathrm{T}}$ where the actuator acts on absolute motion.

Taking the Laplace transform of Eq. (4) and assuming zero initial conditions results in

$$(\mathbf{M}s^2 + \mathbf{K})\mathbf{Q}(\mathbf{s}) = \mathbf{b}F(s). \tag{5}$$

The displacement x that is collocated with the applied force f is related to the vector of generalized displacements $\mathbf{q}$ by the influence vector $\mathbf{b}$ as

$$X(s) = \mathbf{b}^{\mathrm{T}}\mathbf{Q}(s). \tag{6}$$

Combination of Eqs. (5) and (6) gives the transfer function $G(s)$ between the force f and the collocated displacement x:

$$\frac{X(s)}{F(s)} = \mathbf{b}^{\mathrm{T}}(\mathbf{M}s^2 + \mathbf{K})^{-1}\mathbf{b} = G(s). \tag{7}$$

The inverse is written as a function of the determinant and the adjoint, yielding

$$G(s) = \mathbf{b}^{\mathrm{T}} \frac{\mathrm{adj}(\mathbf{M}s^2 + \mathbf{K})}{\det(\mathbf{M}s^2 + \mathbf{K})}\mathbf{b}. \tag{8}$$

The determinant of the denominator is exactly the same determinant that has to be solved for finding the non-trivial solutions of the free response of the undamped structure (Eq. (3)). It can therefore be expressed as

$$\det(\mathbf{M}s^2 + \mathbf{K}) = g_1 \prod_{i=1}^{n} (s^2 + \Omega_i^2), \tag{9}$$

where Ω_i are the resonance frequencies of the undamped structure and g_1 is a constant.

It can be shown that the numerator of Eq. (8) can be written as

$$\mathbf{b}^{\mathrm{T}}\mathrm{adj}(\mathbf{M}s^2 + \mathbf{K})\mathbf{b} = \det(\mathbf{M}_c s^2 + \mathbf{K}_c), \tag{10}$$

where $\mathbf{M}_c$ and $\mathbf{K}_c$ are the mass and stiffness matrices of the constrained structure where the actuator has been replaced by a rigid link. This is easily verified in the case an absolute actuator is acting on the structure. For example, for the three mass system (Fig. 2b), the numerator of Eq. (8) equals

$$\mathbf{b}^{\mathrm{T}}\mathrm{adj}(\mathbf{M}s^2 + \mathbf{K})\mathbf{b} = \det(\mathbf{M}_{2,2} s^2 + \mathbf{K}_{2,2}), \tag{11}$$

where $\mathbf{M}_{2,2}$ and $\mathbf{K}_{2,2}$ are the mass and stiffness matrices of the original structure from which the 2nd row and the 2nd column have been removed. This corresponds to the system with an additional constraint at the degree of freedom the damper acts on.

For the case of a relative actuator this relation might be less clear at first sight, however, we can always change variables such that one of the variables corresponds to the actuator displacement. For the three mass system of Fig. 2a we can change variables for example to $\mathbf{q} = [q_1 \;\; q_2 \;\; q_3 - q_2]^{\mathrm{T}}$, whereby $\mathbf{b} = [0 \;\; 0 \;\; 1]^{\mathrm{T}}$ and the numerator of Eq. (8) equals

$$\mathbf{b}^{\mathrm{T}}\mathrm{adj}(\mathbf{M}s^2 + \mathbf{K})\mathbf{b} = \det(\mathbf{M}_{3,3} s^2 + \mathbf{K}_{3,3}), \tag{12}$$

where $\mathbf{M}_{3,3}$ and $\mathbf{K}_{3,3}$ are the mass and stiffness matrices of the original structure from which the 3rd row and the 3rd column have been removed. Again, this corresponds to a system that is equivalent to the structure for which the actuator is replaced by a rigid link.

So, an equivalent expression as in Eq. (9) can be obtained for the determinant

$$\det(\mathbf{M}_c s^2 + \mathbf{K}_c) = g_2 \prod_{i=1}^{n-1} (s^2 + \omega_i^2), \tag{13}$$

where ω_i are the resonance frequencies of the constrained structure, also called anti-resonance frequencies (Fig. 1b) and g_2 is a constant.

By combination of Eqs. (8)–(10) and (13), the transfer function of the collocated system can be rewritten as

$$G(s) = \frac{g_2}{g_1} \frac{\prod_{i=1}^{n-1} (s^2 + \omega_i^2)}{\prod_{i=1}^{n} (s^2 + \Omega_i^2)}. \tag{14}$$

In system theory, it is a common practice to express transfer functions in this form, in terms of resonance and anti-resonance frequencies [1]. The gain of this transfer function is deduced from the static stiffness of the structure at the location of the actuator κ, by substitution of $s = 0$ in Eq. (14), which gives

$$G(0) = \frac{X(0)}{F(0)} = \frac{1}{\kappa} = \frac{g_2}{g_1} \frac{\prod_{i=1}^{n-1} (\omega_i^2)}{\prod_{i=1}^{n} (\Omega_i^2)} \tag{15}$$

such that the transfer function finally reads

$$G(s) = \frac{1}{\kappa} \frac{\prod_{i=1}^{n} \Omega_i^2}{\prod_{i=1}^{n-1} \omega_i^2} \frac{\prod_{i=1}^{n-1} (s^2 + \omega_i^2)}{\prod_{i=1}^{n} (s^2 + \Omega_i^2)}, \tag{16}$$

where κ can be derived from the stiffness matrix $\mathbf{K}$ by substitution of $s = 0$ in Eq. (7):

$$\kappa = (\mathbf{b}^{\mathrm{T}}\mathbf{K}^{-1}\mathbf{b})^{-1}. \tag{17}$$

3. Eigenvalues of a structure with a single viscous damper

In this section, the possibilities of obtaining the eigenvalues of a structure including a viscous damper are discussed. First, the classical approach is repeated, where solutions are found by solving a quadratic eigenvalue problem. Next it is shown how the eigenvalues can be derived by solving a root locus problem, which is computationally less time consuming. Moreover, the transfer function from which the root locus is computed is composed of parameters that are easily obtainable from any commercial finite element package that offers the opportunity to perform static and modal analysis. The stiffness and mass matrices, required for the classical approach, are not available in all finite element packages. Finally, simple approximate solutions are proposed, which are very useful in the design of dampers.

3.1. Quadratic eigenvalue problem

The force exerted by a viscous damper is proportional to the velocity of the piston, in a direction opposite to the piston motion

$$f = -c\dot{x}, \tag{18}$$

where c is the damping constant.

The free response of a structure including a viscous damper (Fig. 1c) is governed by the equations of motion

$$\mathbf{M}\ddot{\mathbf{q}} + \mathbf{C}\dot{\mathbf{q}} + \mathbf{K}\mathbf{q} = 0, \tag{19}$$

where $\mathbf{C} = c\mathbf{b}\mathbf{b}^{\mathrm{T}}$ is the damping matrix. Non-trivial solutions are found by solving the quadratic eigenvalue problem

$$(\mathbf{M}s^2 + \mathbf{C}s + \mathbf{K})\mathbf{u} = 0, \tag{20}$$

where the eigenvalues are generally complex for a damped structure. They are typically written in the form

$$s = \omega_{n,i}(-\xi_i \pm \mathrm{j}\sqrt{1-\xi_i^2}), \tag{21}$$

where $\omega_{n,i}$ is the modulus of the ith eigenvalue and ξ_i is the modal damping ratio.

3.2. Complex eigenvalues by solving root locus problem

Taking the Laplace transform of Eq. (18) and assuming zero initial conditions gives

$$F(s) = -csX(s). \tag{22}$$

Combination of Eqs. (7) and (22) results in the closed-loop system of the structure with attached viscous damper

$$1 + csG(s) = 0. \tag{23}$$

From this equation it is clear that the root locus of $sG(s)$ shows the effect of changing the damping constant on the poles of the structure with attached viscous damper. Typical examples of such root locus plots are shown in Fig. 3. It is seen that the poles and zeros alternate along the imaginary axis, which is characteristic for an undamped collocated system [1]. It should be clear that in contrast to the resonance frequencies, the values of the anti-resonance frequencies do depend on the location of the damper in the structure and there is always exactly one anti-resonance between two consecutive resonances. For zero damping constant, the closed-loop poles coincide with the undamped resonance frequencies of the structure. Now, increasing the damping

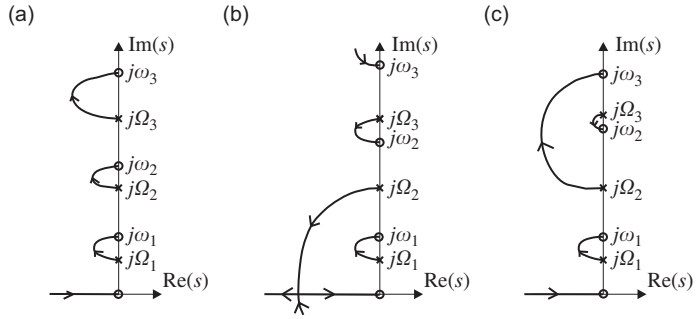

Fig. 3. Typical root locus plots of an undamped discrete structure (degrees of freedom $n>3$) with attached viscous damper for varying damping constant c. (Only the upper half of the s-plane is shown, the diagram is symmetrical with respect to the real axis.)

constant initially increases the modal damping, reaching a maximum value for a particular value of c. In case the mode is critically damped at this point, this mode shall typically remain critically damped by further increasing c, as can be seen for example in Fig. 3b for the second mode. For all the other cases shown in Fig. 3 further increase of c from its optimal value decreases the modal damping and finally it goes to zero for an infinite damping constant. The closed loop poles then coincide with the anti-resonance frequencies of the structure and the damper acts like a support.

Because a viscous damper can only dissipate energy, the branches of the root-locus diagram are all contained in the left half-plane. The form of the root locus diagram of Fig. 3a is typical for situations such as an absolute damper located near the support of a structure, or a relative damper incorporated in the structure. Here, the anti-resonance frequencies differ only slightly from the resonance frequencies and moderate values of modal damping are achieved for the optimal damping constant. As will be seen in the numerical example of a cantilever beam with attached translational viscous damper, in some cases it is possible to achieve critical damping for a mode, as can be seen for example in Fig. 3b for the second mode. Fig. 3c gives an example of a root locus diagram where the third pole is attracted by the second zero, which is very close to this pole. Hereby the branch of the second mode goes to the third zero. It is clearly seen in these examples that the amount of achievable damping is small for poles that have a zero in the near neighborhood and gets larger when they are more separated. When a zero coincides with a pole, the mode is uncontrollable for the corresponding damper location.

3.3. Approximate solution by solving reduced root locus problem

For a given damper location, the exact complex eigenvalues for different values of c are obtained by solving the quadratic eigenvalue problem defined by Eq. (20) for all the values of c. Alternatively, they can be obtained by first solving the two real eigenvalue problems of the undamped structure without and with locked damper and then computing the root locus of $sG(s)$, which is defined by Eq. (23). Although the second method is generally faster than the first method, even this can be computationally time consuming, certainly when the number of degrees of freedom is large. However, solving the root locus for $sG(s)$ with all the poles and zeros is often unnecessary, because mostly we are only interested in the first few modes, while poles and zeros that are far away from the branch of interest have a negligible influence on this branch. By computing the root locus of $sG_p(s)$, where

$$G_p(s) = \frac{1}{\kappa}\prod_{i=1}^{p}\frac{\Omega_i^2(s^2+\omega_i^2)}{\omega_i^2(s^2+\Omega_i^2)} \tag{24}$$

it will be generally sufficient to choose p only a few numbers larger than the number of the mode of interest k to obtain a very good approximation of the exact eigenvalues. This will be demonstrated by numerical examples in Section 4.

3.4. Approximating formulas for the optimal damping

In this section, approximating formulas for the optimal damping constant and maximum modal damping ratio are derived. These are very useful in the design of dampers.

From the knowledge of the values of the poles and zeros, it is not trivial to predict whether a pole will be critically damped, or attracted to one of the zeros. However, it can be stated that it is most probable that a pole will be attracted by the nearest zero. Certainly when the distance is small compared to the other poles and zeros, this probability is large. Because the poles and zeros alternate on the imaginary axis, it should be clear that for the pole that coincides with the kth resonance frequency Ω_k, the nearest zero is the one that coincides with either the subsequent anti-resonance frequency ω_k, or the previous anti-resonance frequency ω_{k-1} (when $k \neq 1$). Because the maximal distance that a zero can be removed from a pole is determined by the distance of this pole to the next (or previous) pole, the closeness of a zero to a pole will be defined here as a fraction of this maximal distance. Therefore, we define

$$\varepsilon_{k1} = \frac{|\Omega_k - \omega_k|}{|\Omega_k - \Omega_{k+1}|} \tag{25}$$

as the relative distance of the kth pole to the subsequent zero compared to the distance of this pole to the subsequent pole. Similarly we define

$$\varepsilon_{k2} = \frac{|\Omega_k - \omega_{k-1}|}{|\Omega_k - \Omega_{k-1}|} \tag{26}$$

as the relative distance of the kth pole to the previous zero compared to the distance of this pole to the previous pole.

Now, two cases can be considered, depending on which of the two distances ε_{k1} or ε_{k2} is smallest. If the distance is sufficiently small and the distance to all the other poles and zeros is large, it will be shown that for both cases approximate values for the eigenvalues can be obtained by solving a reduced root locus problem where only the factors involving the kth pole and the kth or $(k-1)$th zero are retained. From this reduced root locus problem, approximate values for the maximum modal damping and the optimal damping constant can be derived.

3.4.1. Case 1: $\varepsilon_{k1} \leqslant \varepsilon_{k2}$

If we assume that the distance of $j\Omega_k$ to $j\omega_k$ is small compared to the distance to all the other poles and zeros, then Eq. (16) can be simplified in the vicinity of $j\Omega_k$ as follows:

$$G(s)|_{s \approx j\Omega_k} \approx \frac{1}{\kappa_{k,k}} \frac{(s^2 + \omega_k^2)}{(s^2 + \Omega_k^2)} = H_1(s), \tag{27}$$

with

$$\kappa_{p,z} = \kappa \frac{\prod_{i=1}^{z} \omega_i^2}{\prod_{i=1}^{p} \Omega_i^2}. \tag{28}$$

This result is obtained by replacing the factors $(s^2 + w^2)$ where $w = \Omega_1, \ldots, \Omega_{k-1}$ and $w = \omega_1, \ldots, \omega_{k-1}$ by s^2 and replacing the factors $(s^2 + w^2)$ where $w = \Omega_{k+1}, \ldots, \Omega_n$ and $w = \omega_{k+1}, \ldots, \omega_{n-1}$ by w^2.

Substitution of Eq. (27) in Eq. (23) gives

$$1 + csH_1(s) = 1 + \frac{cs}{\kappa_{k,k}} \frac{(s^2 + \omega_k^2)}{(s^2 + \Omega_k^2)} = 0 \tag{29}$$

resulting in typical root locus plots for the individual eigenmodes as in Fig. 4a. This root locus plot can be derived from the root locus plots of Fig. 3 by moving all the poles and zeros that are larger than $j\omega_k$ to infinity and all the poles and zeros that are smaller than $j\Omega_k$ to the origin.

For each eigenmode, there is an optimal value for c that results in maximum modal damping. By substitution of Eq. (21) in Eq. (29), differentiating it with respect to c and assuming that $\partial \xi_i / \partial c = 0$, the

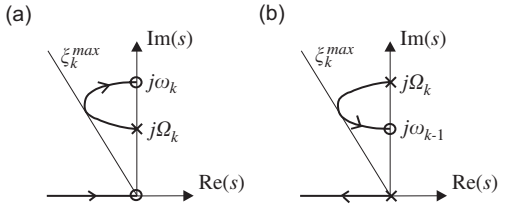

Fig. 4. Root locus of (a) $sH_1(s)$ and (b) $sH_2(s)$.

maximum modal damping and the corresponding optimal damping constant are found:

$$\zeta_k^{\max} = \frac{\omega_k - \Omega_k}{2\Omega_k} \tag{30}$$

and

$$c_k^{\text{opt}} = \kappa_{k,k} \frac{\sqrt{\Omega_k/\omega_k}}{\omega_k}. \tag{31}$$

The maximum modal damping is proportional to the relative spacing of the resonance frequency of the undamped structure and the resonance frequency of the structure with locked damper. This means that the problem of finding a good damper location can be reduced to the problem of finding a location for a rigid link that results in the largest possible increase of the resonance frequency. The importance of inducing such frequency shifts has been demonstrated before for active devices controlled by the IFF algorithm [1], for a taut cable with attached viscous damper [4,9] and for a general discrete structure including viscous dampers [3]. A comparison with the results obtained in this paper is made in Section 5.

3.4.2. Case 2: $\varepsilon_{k1} > \varepsilon_{k2} \quad (k \neq 1)$

If we assume that the distance of $j\Omega_k$ to $j\omega_{k-1}$ is small compared to the distance to all the other poles and zeros, then Eq. (16) can be simplified in the vicinity of $j\Omega_k$ as follows:

$$G(s)|_{s \approx j\Omega_k} \approx \frac{1}{\kappa_{k,k-1}} \frac{(s^2 + \omega_{k-1}^2)}{s^2(s^2 + \Omega_k^2)} = H_2(s). \tag{32}$$

This result is obtained by replacing the factors $(s^2 + w^2)$ where $w = \Omega_1, \ldots, \Omega_{k-1}$ and $w = \omega_1, \ldots, \omega_{k-2}$ by s^2 and replacing the factors $(s^2 + w^2)$ where $w = \Omega_{k+1}, \ldots, \Omega_n$ and $w = \omega_k, \ldots, \omega_{n-1}$ by w^2.

Substitution of Eq. (32) in Eq. (23) gives

$$1 + csH_2(s) = 1 + \frac{c}{\kappa_{k,k-1}} \frac{(s^2 + \omega_{k-1}^2)}{s(s^2 + \Omega_k^2)} = 0 \tag{33}$$

resulting in typical root locus plots for the individual eigenmodes as in Fig. 4b. For each eigenmode, the maximum modal damping and optimal damping constant are

$$\zeta_k^{\max} = \frac{\Omega_k - \omega_{k-1}}{2\omega_{k-1}} \tag{34}$$

and

$$c_k^{\text{opt}} = \kappa_{k,k-1} \Omega_k \sqrt{\Omega_k/\omega_{k-1}}. \tag{35}$$

Note that these formulas are very similar to the formulas of case 1.

3.5. Explicit approximations

An explicit approximate solution for the damping ratio as a function of the damping constant can be useful in practical design situations, because very often suboptimal damping constants are used for reasons of

economy. Such explicit approximations are derived in this section for the two cases considered in the previous section, in a similar way as in Ref. [3].

3.5.1. Case 1: $\varepsilon_{k1} \leqslant \varepsilon_{k2}$

Eq. (29) can be rearranged as follows

$$\frac{(s^2+\Omega_k^2)}{(\Omega_k^2-\omega_k^2)} = \frac{cs/\kappa_{k,k}}{1+cs/\kappa_{k,k}}. \tag{36}$$

Now, small perturbations of the resonance frequencies are assumed:

$$s = \mathrm{j}\Omega_k + \delta_1, |\delta_1| \ll \Omega_k,$$

$$\omega_k = \Omega_k + \delta_2, |\delta_2| \ll \Omega_k, \tag{37}$$

whereby the numerator and the denominator of the left-hand side of Eq. (36) can be approximated by

$$s^2 + \Omega_k^2 \simeq 2\mathrm{j}\Omega_k(s - \mathrm{j}\Omega_k),$$

$$\Omega_k^2 - \omega_k^2 \simeq 2\Omega_k(\Omega_k - \omega_k). \tag{38}$$

Substituting these approximations in Eq. (36) and assuming that $s = \mathrm{j}\omega_k$ in the right-hand side of Eq. (36) gives an explicit approximate solution for the eigenvalues

$$s = \mathrm{j}\Omega_k + (\Omega_k - \omega_k)\frac{\eta_k}{1+\mathrm{j}\eta_k}, \tag{39}$$

where the non-dimensional damping constant η_k is defined by

$$\eta_k = \frac{c\omega_k}{\kappa_{k,k}}. \tag{40}$$

Eq. (39) is the same as the explicit approximate solution obtained by Main and Krenk [3], only the value of η_k is different. Krenk derived previously explicit approximations in the same form for the special case of a taut cable [4] and a beam with rotational viscous dampers at the end [5].

An explicit equation for the damping ratio can be deduced from Eq. (39) by dividing the negative real part of the eigenvalue by its absolute value:

$$\xi_k = \frac{-\mathrm{Re}(s)}{|s|} = \frac{(\omega_k - \Omega_k)\eta_k}{\sqrt{(\eta_k^2\omega_k^2 + \Omega_k^2)(1+\eta_k^2)}}. \tag{41}$$

3.5.2. Case 2: $\varepsilon_{k1} > \varepsilon_{k2}$ $(k \neq 1)$

Explicit approximating solutions can be derived in a similar way as for case 1. This results in equations of exactly the same form as Eq. (39) and Eq. (41), only ω_k should be replaced by ω_{k-1} and η_k is defined by

$$\eta_k = \frac{c}{\kappa_{k,k-1}\Omega_k}. \tag{42}$$

4. Cantilever beam example

The correctness of the foregoing approximate solutions of the eigenvalues is verified by means of numerical examples for a cantilever Bernouilli–Euler beam of length l with a viscous damper attached at a distance a from the clamping point, as depicted in Fig. 1c. The quadratic eigenvalue problem Eq. (20) for a beam with mass per unit length m and bending stiffness EI, discretizated by n finite elements is expressed in non-dimensional form as

$$(\mathbf{M}_b\tilde{s}^2 + \tilde{c}\ \mathbf{b}\mathbf{b}^{\mathrm{T}}\tilde{s} + \mathbf{K}_b)\mathbf{u} = 0, \tag{43}$$

where $\tilde{s} = s\sqrt{ml^4/EI}$ are the non-dimensional complex eigenvalues, $\mathbf{u} = [v_1\ \theta_1\ \cdots\ v_n\ \theta_n]^{\mathrm{T}}$ are the corresponding modeshapes consisting of one translational degree of freedom v_k and one rotational degree

of freedom θ_k for each node k and $\tilde{c} = cl/\sqrt{mEI}$ is the non-dimensional damping constant. The stiffness and mass matrices $\mathbf{K}_b$ and $\mathbf{M}_b$ are given in Appendix A. The number of beam elements is chosen 50 for the following numerical examples, resulting in a total of 100 degrees of freedom. Hereby the first fifteen eigenvalues are converged within an error of 0.1% of their asymptotic values.

Two cases are considered for this numerical example: a beam with a damper acting on the translational degrees of freedom v and on the rotational degrees of freedom θ.

4.1. Cantilever beam with translational viscous damper

The exact solution of the modal damping ratio is compared to the approximate solutions in Fig. 5 for the first three modes of a cantilever with a translational damper located at $a/l = 0.06$ and 0.2. It is seen that the solutions obtained by solving the root locus of $sG_p(s)$ where $G_p(s)$ is defined by Eq. (24) are visibly indistinguishable from the exact solution for all cases when only three extra pole-zero pairs are considered above the pole-zero pair corresponding to the mode of interest.

Fig. 5 also shows explicit approximations defined by Eq. (41). It is clear that these are very accurate when the difference in eigenvalues between the undamped case and the constrained case are small, which is true for small values of a/l. For larger values of a/l the accuracy of the explicit approximations reduces.

Also plotted in Fig. 5 are the the solutions for the root locus of $sH_1(s)$, defined by Eq. (29). The optimum of these curves corresponds to the approximating formulas for the maximum modal damping (Eq. (30)) and the optimal damping constant (Eq. (31)). The equations off case 1 are used here, because for all three modes the subsequent zeros are closer to the corresponding pole than the previous zeros for a damper located at $a/l = 0.06$ and 0.2, as can be seen in Fig. 6a. The approximations are very good for all cases, except for the case of Fig. 5f. This can be explained by the fact that the closest zero is relatively far away from the pole for this case, which seems to be critically damped for values of c larger than a certain critical value.

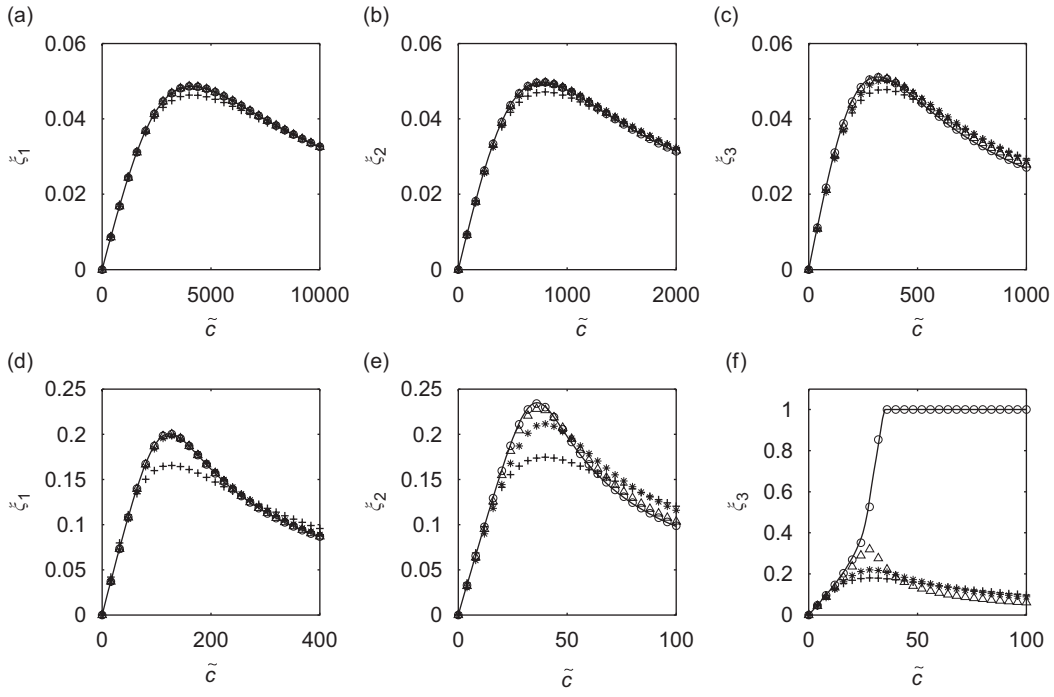

Fig. 5. Modal damping ratio for a cantilever beam with translational damper. Exact, —; explicit approximation Eq. (41), +; approximation by root locus of $sG_{k+1}(s)$, △; approximation by root locus of $sG_{k+3}(s)$, ○; approximation by root locus of $sH_1(s)$, ∗. (a) Mode 1, $a/l = 0.06$; (b) mode 2, $a/l = 0.06$; (c) mode 3, $a/l = 0.06$; (d) mode 1, $a/l = 0.2$; (e) mode 2, $a/l = 0.2$; (f) mode 3, $a/l = 0.2$.

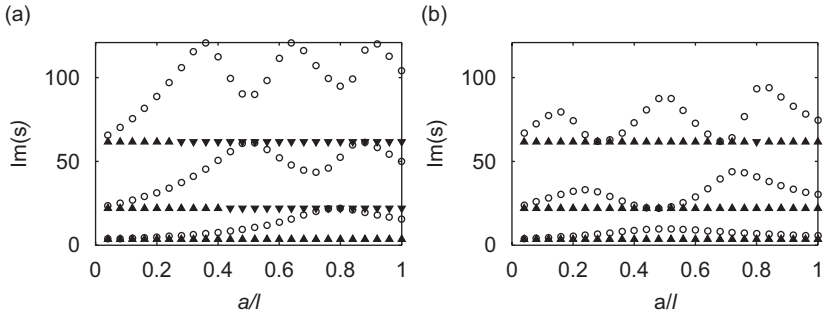

Fig. 6. Location of the poles (if $\varepsilon_{1k} \leqslant \varepsilon_{2k}$, ▲; if $\varepsilon_{2k} < \varepsilon_{1k}$, ▼) and zeros (○) on the imaginary axis in the s-plane for a cantilever beam with translational damper (a) and rotational damper (b).

Computation of the exact and approximate solutions of the eigenvalues is repeated for different values of the damper location a/l. The maximum modal damping ratios obtained by the approximating formulas for case 1 (Eq. (30)) and case 2 (Eq. (34)) are compared with the exact optimal values in Fig. 7. It is seen that if the closest zero is located within a margin of 45% of its maximal possible distance, the approximations are very good (this situation is indicated by a marker that is filled black in Fig. 7). Over the larger part of the beam, good approximations are found, except for the regions where the modes are critically damped. It should be noted here, that the root locus diagram for a cantilever beam with a translational damper has the form depicted by Fig. 3b. There is always one mode that is critically damped, while modes with a higher mode number fulfill the condition of case 2 and modes with a lower mode number fulfill the condition of case 1. The number of the mode that is critically damped increases with a decreasing value of a/l.

The exact optimal values of the damping constant are compared to the approximations for case 1 and case 2 by, respectively, Eq. (31) and Eq. (35) in Fig. 8. For damper locations where a mode can be critically damped, the minimal value of c for which critical damping is achieved is plotted here. As for the prediction of the optimal damping constant, it is seen that when the closest zero is located within a relative distance of 0.45 compared to the distance of the next (or previous) pole, the difference between the approximate damping constant and the exact value is very small. The largest differences are visible at locations where the maximum modal damping approaches zero, thus the least interesting regions. And even here, the maximal difference is smaller than 2 dB, which coincides with a factor 1.26. Because of the typical robust character of the modal damping versus the damping constant at the optimal point, as illustrated for example in Fig. 5, a difference of this magnitude results in a modal damping ratio that is very close to its optimal value. Note that if no restriction would be made on the allowed relative distance of the considered pole and zero, the prediction of the optimal damping constant would be good over the entire range of the beam length, even in regions where critical damping is achieved. The error on the approximate value of the damping constant for the case the formulas of the closest zero are used, is smaller than 2 dB over the entire beam length.

4.2. Cantilever beam with rotational viscous damper

The same calculations are repeated here for a cantilever beam with attached absolute rotational viscous damper. In contrast to the previous example, the subsequent zeros are always closer here than the previous zeros, as shown in Fig. 6b. The root locus plots all have the form of Fig. 3a.

As depicted in Fig. 9, the approximate values of the maximum modal damping are in very good agreement with the exact values, except for a small region at the end of the beam for the second and third mode. For this example too, a good approximation is guaranteed when the distance of the closest zero to the pole is smaller than 45% of the distance to the next (or previous) pole. This can also be concluded for the prediction of the optimal damping constant (Fig. 10). The largest difference in the region at the end of the beam for mode two and three is smaller than 3 dB, which coincides with a factor 1.41. Again in these regions the maximum modal damping approaches zero. And again the prediction of the optimal damping constant would be good over the

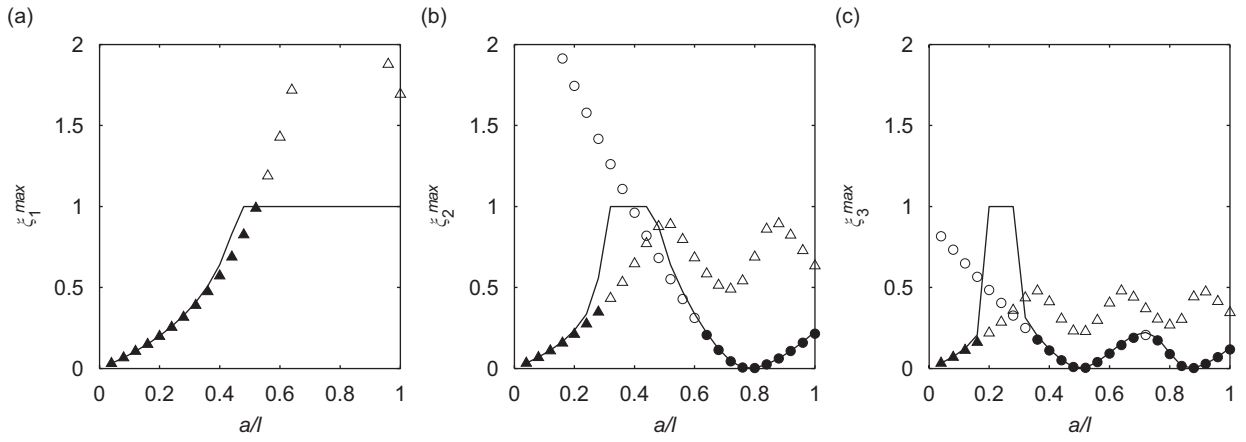

Fig. 7. Maximum modal damping for beam with translational damper. Exact, —; approximating formula of case 1, triangles: if $\varepsilon_{1k} \leqslant \varepsilon_{2k}$ and $\varepsilon_{1k} \leqslant 0.45$, ▲, otherwise, △; approximating formula of case 2, circles: if $\varepsilon_{2k} < \varepsilon_{1k}$ and $\varepsilon_{2k} \leqslant 0.45$, •; otherwise, ○. (a) Mode 1; (b) mode 2; (c) mode 3.

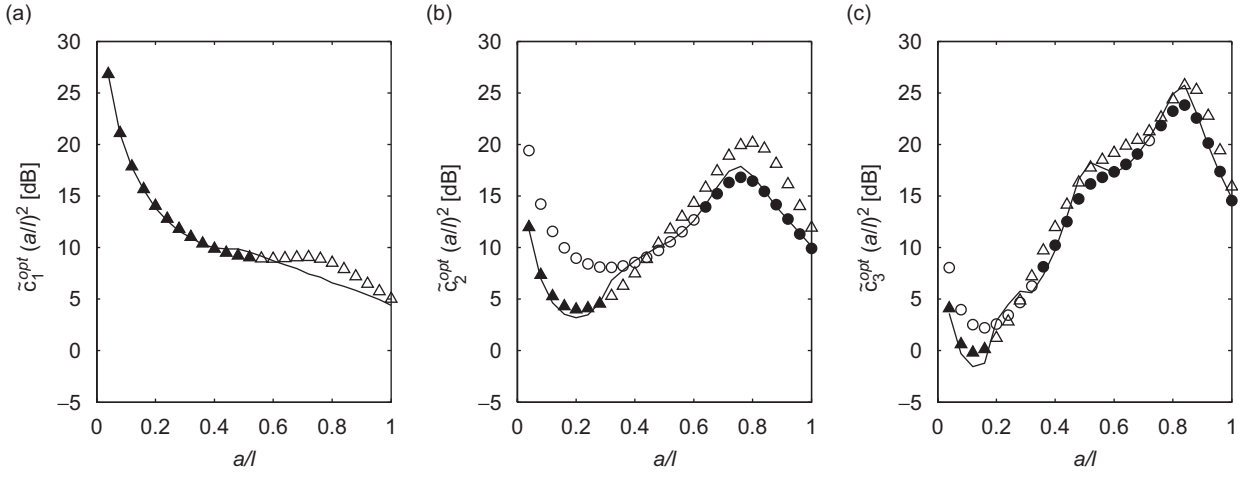

Fig. 8. Optimal damping constant for beam with translational damper. Exact, —; approximating formula of case 1, triangles: if $\varepsilon_{1k} \leqslant \varepsilon_{2k}$ and $\varepsilon_{1k} \leqslant 0.45$, ▲, otherwise, △; approximating formula of case 2, circles: if $\varepsilon_{2k} < \varepsilon_{1k}$ and $\varepsilon_{2k} \leqslant 0.45$, •; otherwise, ○. (a) Mode 1; (b) mode 2; (c) mode 3.

entire beam length if no restriction would be made on the allowed relative distance of the considered pole and zero. So, actually the results of this example confirm the results of the previous example.

5. Comparison with previous research

The approximate solutions for the complex eigenvalues and the formulas for the optimal damping are very similar to results obtained in the work of Preumont [1] and Main and Krenk [3]. In this paper however, an alternate approach is used, which leads to new insights. A comparison is made in this section.

The most striking difference is that this paper presents two approximations, depending on whether the root locus terminates at the kth or the $(k-1)$th anti-resonance frequency, while in Refs. [1,3] only one case is considered, i.e. the case where the root locus terminates at the kth anti-resonance frequency. On the other hand, it should be clear that the method represented in this paper is restricted to a single damper, while the works of Preumont [1] and Main and Krenk [3] propose solutions where multiple devices are used. Moreover,

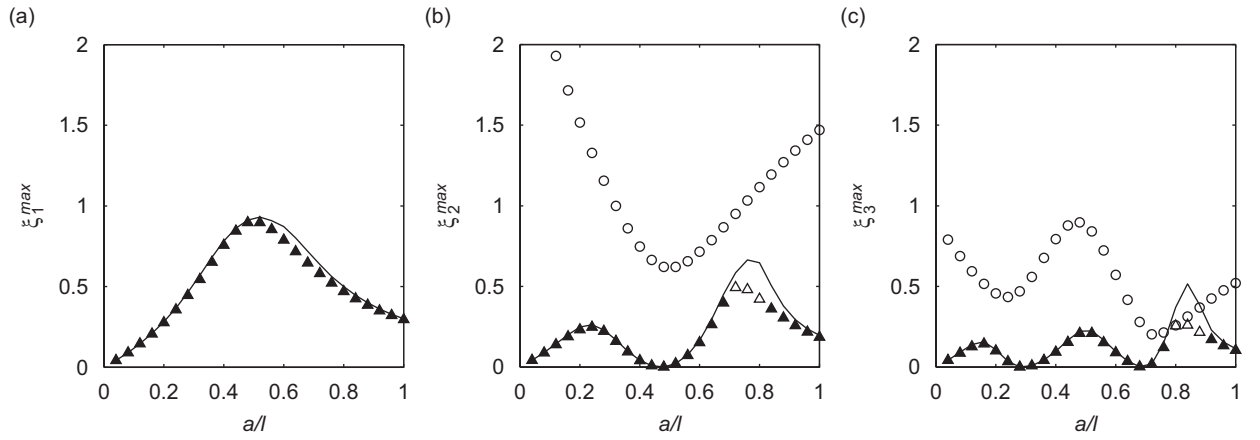

Fig. 9. Maximum modal damping for beam with rotational damper. Exact, —; approximating formula of case 1, triangles: if $\varepsilon_{1k} \leqslant \varepsilon_{2k}$ and $\varepsilon_{1k} \leqslant 0.45$, ▲, otherwise, △; approximating formula of case 2, circles: if $\varepsilon_{2k} < \varepsilon_{1k}$ and $\varepsilon_{2k} \leqslant 0.45$, •; otherwise, ○. (a) Mode 1; (b) mode 2; (c) mode 3.

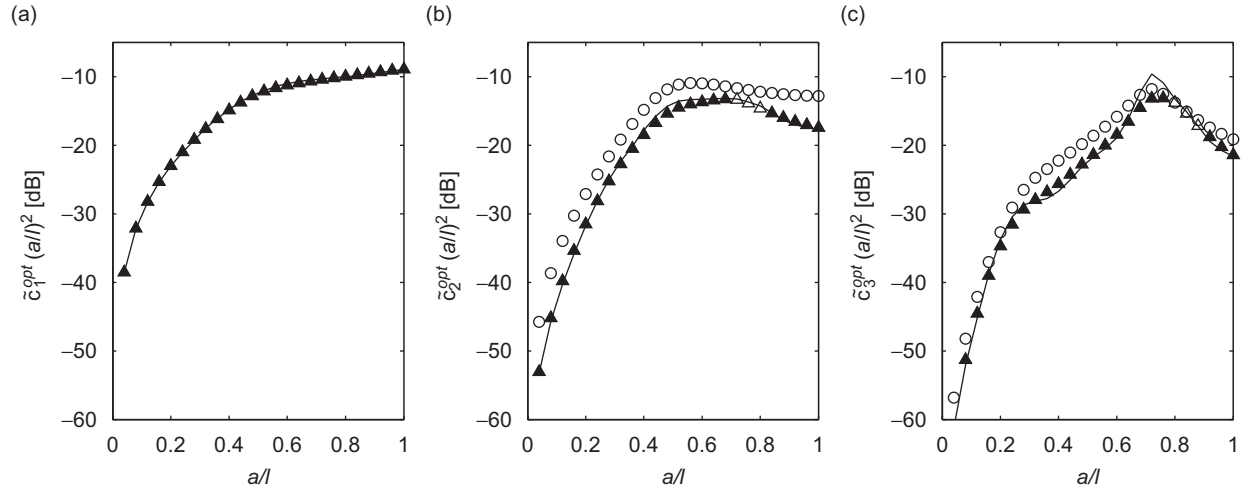

Fig. 10. Optimal damping constant for beam with rotational damper. Exact, —; approximating formula of case 1, triangles: if $\varepsilon_{1k} \leqslant \varepsilon_{2k}$ and $\varepsilon_{1k} \leqslant 0.45$, ▲, otherwise, △; approximating formula of case 2, circles: if $\varepsilon_{2k} < \varepsilon_{1k}$ and $\varepsilon_{2k} \leqslant 0.45$, •; otherwise, ○. (a) Mode 1; (b) mode 2; (c) mode 3.

in contrast to Ref. [3], no solution for obtaining the modeshapes is presented in this paper. Whereas these are obviously the most remarkable differences, the discussion below reveals some other important differences.

Preumont [1] investigated the effect of active devices controlled with the integral force feedback control algorithm, which is equivalent to viscous damping. By using a diagonalization technique, Preumont found equations with exactly the same form as Eq. (29)[1] for a truss structure with piezoelectric actuators (Eqs. (5.38) and (13.31) in Ref. [1]) and tendon control of cable structures with active devices (Eq. (14.14) in Ref. [1]). The equations have exactly the same form, only $\kappa_{k,k}$ is replaced in Ref. [1] by, respectively, the stiffness of the active struts and the stiffness of the cables for the two studied cases. Very important is that the approximations obtained in Ref. [1] are only valid for the special case where a series connection of a spring and a damper is

[1]The equations of Ref. [1] are equivalent to Eq. (29) and not Eq. (33). The usage of the symbols ω_k and Ω_k is reversed here in comparison with Ref. [1].

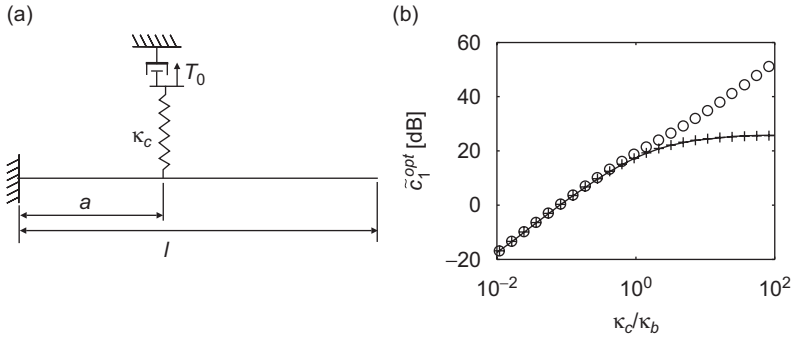

Fig. 11. (a) Cable stayed cantilever beam with damper at the cable support. (b) Optimal damping constant of the first mode, a/l = 0.4. Exact, —; approximation by Eq. (44), ○; approximation by Eq. (31), +.

included in the structure, while the approximations obtained in the present paper are valid for the general case where a damper is included in the structure. According to the authors it is not possible to use the same diagonalization technique as in Ref. [1] to obtain similar approximations for the general case.

Now, let us consider the example of a cantilever beam with a cable attached at a relative distance a/l from the clamping point. The cable pre-tension is T_0 and a damper is placed between the cable and the support as depicted in Fig. 11a. As in Section 14.5 of Ref. [1], the dynamics of the cable are neglected such that the cable behaves like a bar with stiffness κ_c. The approximate formulas for the maximum modal damping ratio derived by Preumont (Eq. (14.15)) are exactly the same as the formulas obtained in the present paper (Eq. (30)). However, the corresponding optimal damping constant is different. Preumont suggests a value of

$$c_k^{\mathrm{opt}} = \kappa_c \frac{\sqrt{\Omega_k/\omega_k}}{\omega_k}, \tag{44}$$

where κ_c is the cable stiffness. It should be clear that this value is only correct when κ_c is smaller than the stiffness of the beam at the attachment point of the cable κ_b. This is confirmed by the graph of Fig. 11b, which compares the optimal damping constant obtained from Eq. (44) with the exact value for different values of the cable stiffness. If we compare the exact value with the optimal damping constant obtained in the present paper (Eq. (31)), we can see that there is a very good agreement, even for values of κ_c that are larger than κ_b. For the examples considered in Ref. [1], the condition $\kappa_c < \kappa_b$ is satisfied, such that Eq. (44) is applicable. If for an other problem this would not be the case, the approximations of the present paper should be used.

While both in the present paper and in the work of Preumont [1] the problem is treated from a control point of view, Main and Krenk [3] used a different approach, where an approximate solution to the complex eigenproblem was obtained by assuming a linear interpolation between the solutions of the undamped eigenproblem and the constrained eigenproblem with rigid links at the dampers. This resulted in a quartic equation (Eq. (28) in Ref. [3]) which can be solved iteratively. This equation was further simplified by assuming small perturbations of the eigenfrequencies, leading to a cubic equation (Eq. (38) in Ref. [3]) with exactly the same form as Eq. (29) of this paper, except that $\kappa_{k,k}$ is replaced in this reference by $(\omega_k^2 - \Omega_k^2)/(\mathbf{b}^{\mathrm{T}}\mathbf{u}_k)^2$ for the case of a single damper, where $\mathbf{u}_k$ is the mass normalized modeshape of the kth undamped eigenmode. The value of $\kappa_{k,k}$ is not exactly the same as the value of $(\omega_k^2 - \Omega_k^2)/(\mathbf{b}^{\mathrm{T}}\mathbf{u}_k)^2$. These values influence the scaling factor of the damping constant, so the prediction of the optimal damping constant is different with both values. Fig.12 shows that the difference is small for the numerical examples of the cantilever beam in the region of interest, which is the region where the kth anti-resonance frequency is relatively close to the kth resonance frequency. So, the approximate solutions are similar, but a formulation in terms the static stiffness at the damper location might be preferred over a formulation in terms of the mass normalized modeshape. The static stiffness is easily obtainable from most commercial finite element software packages and is also easily experimentally identifiable. Certainly when damping is introduced in the structure by incorporating a hinge in the structure and placing a spring and damper in parallel at the created degree of freedom, a representation of

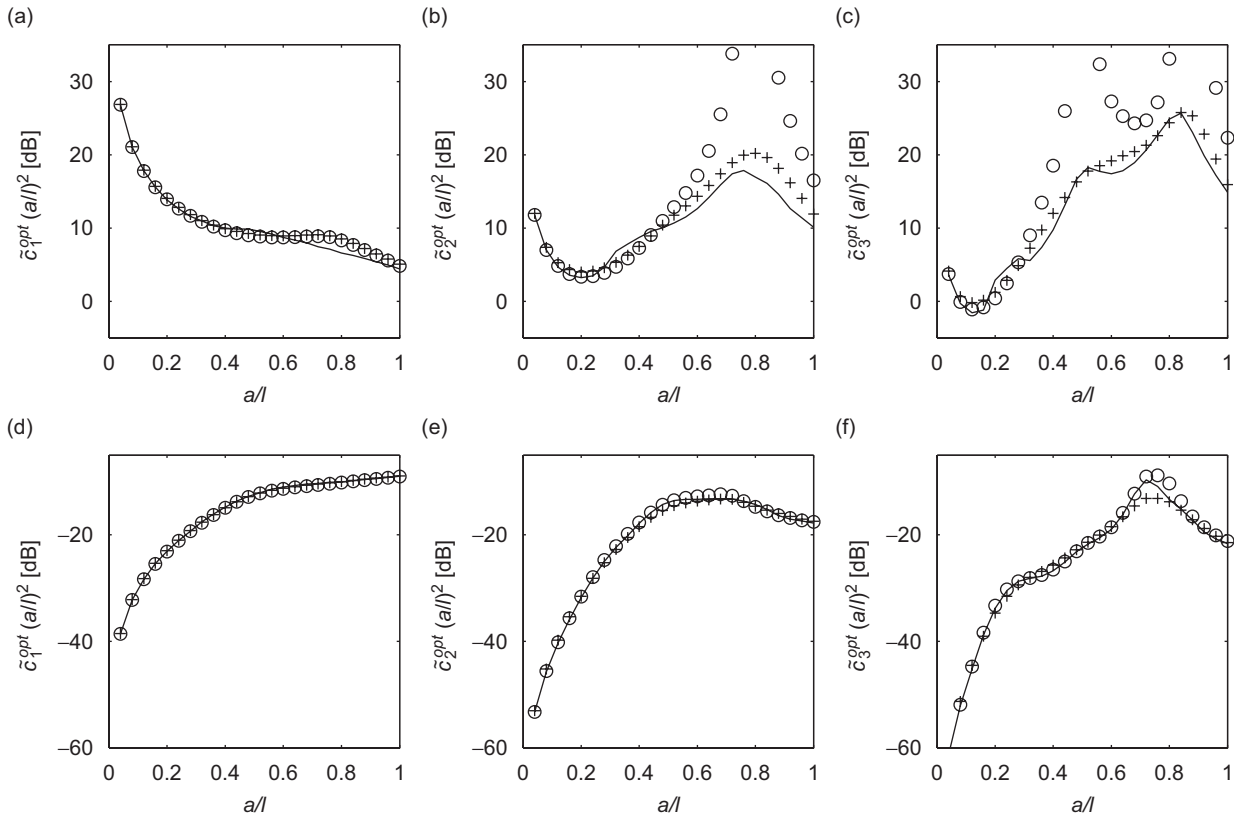

Fig. 12. Optimal damping constant. Exact, —; approximating formula of case 1, +; approximating formula of case 1 where $\kappa_{k,k}$ is replaced by $(\omega_k^2 - \Omega_k^2)/(\mathbf{b}^T\mathbf{u}_k)^2$, ○. (a) Mode 1, translational damper; (b) mode 2, translational damper; (c) mode 3, translational damper; (d) mode 1, rotational damper; (e) mode 2, rotational damper; (f) mode 3, rotational damper.

results in terms of the static stiffness is interesting, since the static stiffness is equal to the spring stiffness in that case. Damping is introduced in this way for example in spray boom structures [10].

The explicit expression (39) is derived here in an equivalent way as in Ref. [3]. However, formulas for the optimal damping are not obtained from this explicit expression as given in Ref. [3]. They are derived here directly from the more accurate Eq. (29), in a similar way as in Ref. [1]. The optimum of the explicit expression corresponds to:

$$\eta_k = \sqrt{\Omega_k/\omega_k}, \quad \xi_k = \frac{\omega_k - \Omega_k}{\omega_k + \Omega_k}. \tag{45}$$

It is shown in Figs. 13 and 14 that the approximations corresponding to Eq. (45) are only accurate for small values of a/l. This is explained by the fact that the explicit expression was derived subject to assumptions of small perturbations of the eigenfrequencies. Judging from the location of the poles and zeros in Fig. 6, this assumption is only valid for small values of a/l. For larger values of a/l the assumption of small perturbations is clearly violated, such that the approximations are compared here outside their range of applicability. In fact, Main and Krenk [3] suggested to optimize the decay rate $\xi_k\omega_{n,k}$ of the explicit expression instead of the modal damping ratio. The maximum decay rate coincides with the values:

$$\eta_k = 1, \quad \xi_k\omega_{n,k} = \frac{\omega_k - \Omega_k}{2}, \quad \xi_k = \frac{\omega_k - \Omega_k}{\sqrt{2}\sqrt{\omega_k^2 + \Omega_k^2}}. \tag{46}$$

However, from Figs. 13 and 14 it is clear that the values which maximize the decay rate are only slightly different from the values which maximize the modal damping ratio, certainly for small values of a/l. Now, the

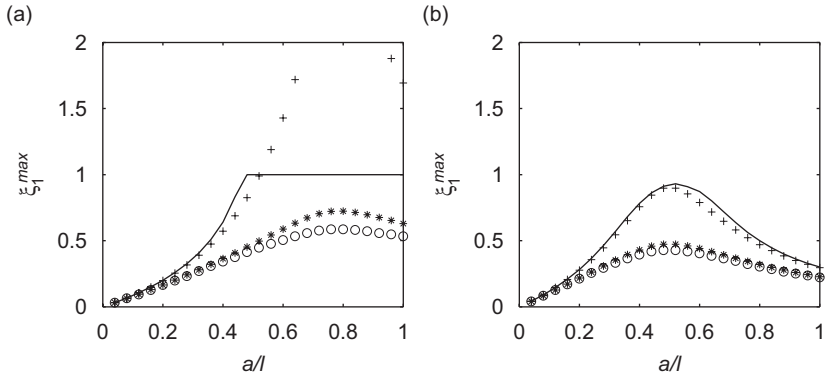

Fig. 13. Maximum damping ratio. Exact, —; approximating formula of case 1 (Eq. (30)), +; approximating formula of Eq. (45), ∗; approximating formula of Eq. (46), ○. (a) mode 1, translational damper; (b) mode 1, rotational damper.

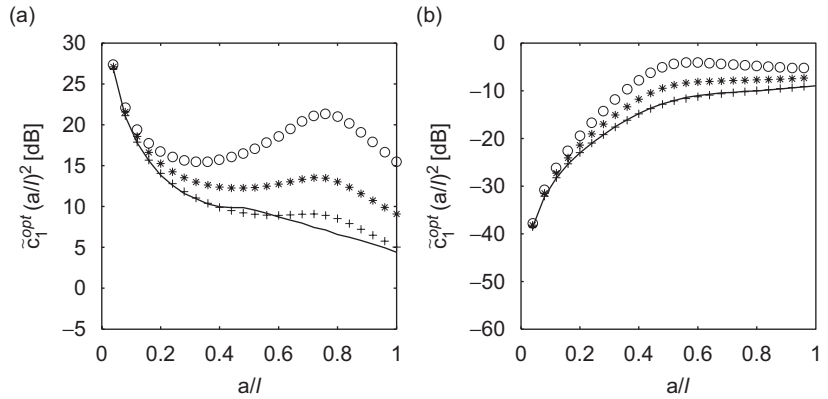

Fig. 14. Optimal damping constant. Exact, —; approximating formula of case 1 (Eq. (31)), +; approximating formula of Eq. (45), ∗; approximating formula of Eq. (46), ○. (a) Mode 1, translational damper; (b) mode 1, rotational damper.

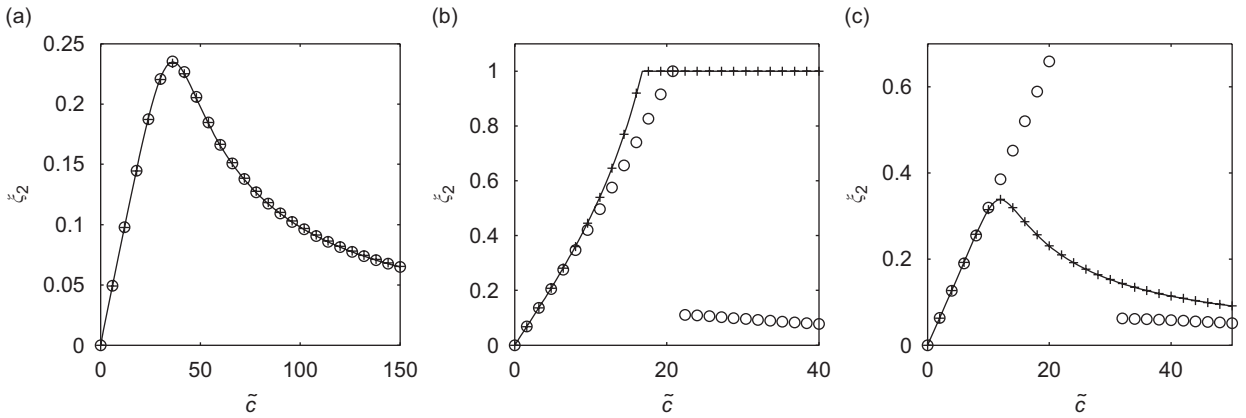

Fig. 15. Modal damping ratio for a cantilever beam with translational damper. Exact, —; approximation by root locus of $sG_{k+3}(s)$, +; approximation by iterative scheme of Ref. [3], ○. (a) Mode 2, $a/l = 0.2$; (b) mode 2, $a/l = 0.4$; (c) mode 2, $a/l = 0.6$.

formulas for the optimal damping derived in the present paper (Eqs. (30)–(31)) are obtained directly from Eq. (29), which is more accurate than the explicit expression (39). This explains why the new approximations are accurate over a broader range, as illustrated in Figs. 13 and 14.

The quartic equation derived by Main and Krenk (Eq. (28) in Ref. [3]) can be solved iteratively to obtain solutions for the complex eigenvalues with a better accuracy than those obtained from the explicit expression. Fig. 15a shows that the iterative scheme converges to the exact solution as long as the root-locus is of the form of Fig. 3a, i.e. the poles are attracted by the subsequent zeros. In case a pole is attracted by the previous zero, or critical damping is achieved, the iterative scheme no longer converges to the exact solution, as depicted in Figs. 15b and c, while the approximate solution with the reduced root locus represented in Section 3.3 does converge to the exact solution.

6. Conclusion

The complex eigenvalues of a flexible structure including a viscous damper are derived by solving the root locus of a transfer function that is composed of easily identifiable parameters: the static stiffness of the structure at the damper location, the resonance frequencies of the undamped structure and the resonance frequencies of the structure in which the damper is replaced by a rigid link. Exact solutions are obtained by taking all the resonance frequencies and anti-resonance frequencies into account. Since for structures with a large number of degrees of freedom computation time can be large, an approximate solution is proposed where only a limited number (p) of resonance frequencies and anti-resonance frequencies are considered. For numerical examples of a cantilever beam with attached viscous damper, it was shown that taking $p = k + 3$, where k is the mode number of the mode of interest, is sufficient to obtain a good approximation.

Approximating formulas are derived for the maximum modal damping ratio and the corresponding optimal damping constant. For a given mode, the maximal attainable damping ratio is proportional to the relative spacing of the resonance frequency of the undamped structure and the closest resonance frequency of the structure with locked damper. This means that the problem of finding a good damper location can be reduced to the problem of finding a location for a rigid link that results in the largest deviation of the closest resonance frequency. This is an extension to the classical statement that achievable damping is proportional to the induced frequency shift in the sense that the closest anti-resonance frequency is taken into account and not only the subsequent anti-resonance frequency.

The correctness of the predicted value of the maximum modal damping ratio for the kth mode can be checked by computing the relative distance of the kth resonance frequency to the closest anti-resonance frequency (ε_{k1} or ε_{k2}). This value should be sufficiently small to ensure a good approximation. For the considered numerical examples it is seen that a value smaller than 0.45 is sufficient. In fact this means that a good prediction of the modal damping ratio is only ensured when the achievable amount of damping is limited. This may seem contradictory, but in many cases it is not possible to obtain large damping ratios, because of practical considerations. This is for example the case for damping of a taut cable where the distance of the damper attachment point to the end of the cable should be small. On the other hand, it is shown in the numerical examples of this paper, that fairly high levels of modal damping can be predicted very well, certainly for the lowest mode of vibration, which is often the mode of interest.

Because of the typical robust character of the modal damping versus the damping constant at the optimal point, the prediction of the optimal damping constant is not very critical. For the considered numerical examples of a cantilever beam with attached translational or rotational damper, the approximating formulas give a good prediction of the optimal damping constant of the first three modes for all possible damper locations.

The approximate solutions for the complex eigenvalues presented in this paper are very similar to existing approximations obtained in Refs. [1,3]. A thorough comparison revealed that the new approximations, obtained with the root-locus method, are applicable in a broader range, without losing simplicity. On the other hand, it should be mentioned that the method represented in this paper is restricted to a single damper, while Refs. [1,3] also propose solutions for the case multiple devices are used.

7. Acknowledgments

The authors want to express their gratitude to the Interuniversity Attraction Poles program (Belgian Science Policy) and the FWO Vlaanderen (Fund of Scientific Research Flanders) for their financial support.

Appendix A. Stiffness and mass matrices for cantilever beam

The stiffness and mass matrices that appear in the non-dimensional form of the quadratic eigenvalue problem Eq. (43) of a cantilever beam, discretizated by n finite elements of section length $h = l/n$ are, respectively,

$$\mathbf{K}_b = n^3 \begin{bmatrix} \mathbf{K}_{11}+\mathbf{K}_{22} & \mathbf{K}_{12} & & \\ \mathbf{K}_{12}^{\mathrm{T}} & \mathbf{K}_{11}+\mathbf{K}_{22} & \mathbf{K}_{12} & \\ & \ddots & & \\ & \mathbf{K}_{12}^{\mathrm{T}} & \mathbf{K}_{11}+\mathbf{K}_{22} & \mathbf{K}_{12} \\ & & \mathbf{K}_{12}^{\mathrm{T}} & \mathbf{K}_{22} \end{bmatrix} \tag{A.1}$$

and

$$\mathbf{M}_b = \frac{1}{420n} \begin{bmatrix} \mathbf{M}_{11}+\mathbf{M}_{22} & \mathbf{M}_{12} & & \\ \mathbf{M}_{12}^{\mathrm{T}} & \mathbf{M}_{11}+\mathbf{M}_{22} & \mathbf{M}_{12} & \\ & \ddots & & \\ & \mathbf{M}_{12}^{\mathrm{T}} & \mathbf{M}_{11}+\mathbf{M}_{22} & \mathbf{M}_{12} \\ & & \mathbf{M}_{12}^{\mathrm{T}} & \mathbf{M}_{22} \end{bmatrix}, \tag{A.2}$$

where

$$\mathbf{K}_{11} = \begin{bmatrix} 12 & 6h \\ 6h & 4h^2 \end{bmatrix}, \quad \mathbf{K}_{12} = \begin{bmatrix} -12 & 6h \\ -6h & 2h^2 \end{bmatrix}, \quad \mathbf{K}_{22} = \begin{bmatrix} 12 & -6h \\ -6h & 4h^2 \end{bmatrix} \tag{A.3}$$

and

$$\mathbf{M}_{11} = \begin{bmatrix} 156 & 22h \\ 22h & 4h^2 \end{bmatrix}, \quad \mathbf{M}_{12} = \begin{bmatrix} 54 & -13h \\ 13h & -3h^2 \end{bmatrix}, \quad \mathbf{M}_{22} = \begin{bmatrix} 156 & -22h \\ -22h & 4h^2 \end{bmatrix}. \tag{A.4}$$

References

[1] A. Preumont, *Vibration Control of Active Structures: An Introduction*, second ed., Kluwer, Dordrecht, 2002.
[2] T.T. Soong, B.F. Spencer, Supplemental energy dissipation: state-of-the-art and state-of-the practice, *Engineering Structures* 24 (2002) 243–259.
[3] J.A. Main, S. Krenk, Efficiency and tuning of viscous dampers on discrete systems, *Journal of Sound and Vibration* 286 (2005) 97–122.
[4] S. Krenk, Vibrations of a taut cable with an external damper, *Journal of Applied Mechanics* 67 (2000) 772–776.
[5] S. Krenk, Complex modes and frequencies in damped structural vibrations, *Journal of Sound and Vibration* 270 (2004) 981–996.
[6] J.R. Høgsberg, S. Krenk, Linear control strategies for damping of flexible structures, *Journal of Sound and Vibration* 293 (2006) 59–77.
[7] M. Gürgöze, H. Erol, Dynamic response of a viscously damped cantilever with a viscous end condition, *Journal of Sound and Vibration* 298 (2006) 132–153.
[8] D. Cha, A general approach to formulating the frequency equation for a beam carrying miscellaneous attachments, *Journal of Sound and Vibration* 286 (2005) 921–939.
[9] J.A. Main, N.P. Jones, Free vibrations of taut cable with attached damper. I: Linear viscous damper, *Journal of Engineering Mechanics* 128 (2002) 1062–1071.
[10] K. Engelen, H. Ramon, J. Anthonis, Damping of spray boom structures with non-linear dampers, *Proceedings of ISMA 2006 International Conference on Noise and Vibration Engineering*, Leuven, Belgium, September 2006, pp. 147–156.